MS NO. acp-2015-385

We are grateful for the reviewer's comments. Those comments are all valuable and helpful for improving our paper. We answered the comments carefully and have made corrections in the submitted manuscript. The corrections and the responses are as following:

1. Authors discuss nitrate as coating materials on sea-salt particles in several sections (e.g., 4.1). However, there is no N signal in Figures 3-5, and authors mention that "N content cannot be directly measured but has been inferred based on the probable aerosol components". If substantial amounts of nitrate occur within the particles, N peak may arise between C and O in the EDX signals (e.g., Fig. 4 h and j), although it depends on the detection efficiency and the energy resolution on the EDX. I cannot see N in the mapping data in Fig. 7. SIMS data in Fig. 8 does not show the presence of nitrate as well. Although theoretically it will be likely that nitrate occurs on the coating, the main discussion should not be based on "the probable aerosol components." I suggest distinguishing between the result and discussion clearly, i.e., nitrate should be discussed only in the discussion with proper references. Also the occurrence of nitrate is not a direct evidence, and the relative sentences need to be revised (e.g., Page 16727 line 23).

Response 1: We appreciate the reviewer's comments. Also, we noticed there is absent about nitrate evidence in the ACPD paper. Based on the reviewer's comments, we carefully added new nanoSIMS experiments. Firstly, we generated laboratory $NaNO_3$ particles on silicon substrate. The new Figure S3 shows the $^{14}N^{16}O_2^-$ and $^{23}Na^{16}O^-$ can be good markers of $NaNO_3$. Secondly, we used these markers to analyze the ambient SSA particles. Ion mappings and line scans show that these aged SSA contain abundant $^{14}N^{16}O_2^-$ and $^{23}Na^{16}O^-$ instead of fresh SSA (Fig. 9). Therefore, we can make one solid conclusion which the aged SSA contain $NaNO_3$.

We have revised the text in section 2.3 as follows:

"Laboratory generated $NaNO_3$ particles on silicon substrate analyzed by nanoSIMS show that $^{14}N^{16}O_2^-$ and $^{23}Na^{16}O^-$ are their markers (Fig. S3)."

We have revised the text in section 4.1 as follows:

“Figure 9a shows $^{35}Cl^-$ in the NaCl core and minor $^{16}O^-$ and $^{32}S^-$ in the coating in fresh SSA. Figure 9b shows the absence of $^{35}Cl^-$ and the high intensity of $^{16}O^-$, $^{14}N^{16}O_2^-$, $^{32}S^-$, and $^{23}Na^{16}O^-$ in fully aged SSA. These results are completely consistent with the TEM and STEM observations in Figures 2, 4, and 8. Based on the mappings of $^{32}S^-$ (sulfate), $^{14}N^{16}O_2^-$ (nitrate), and $^{23}Na^{16}O^-$ in Figure 9, the nanoSIMS analysis provide direct evidence of Na_2SO_4 and $NaNO_3$ formation in fully aged SSA.”

We have revised the text (Page 16727, line 23) as follows:

“Integrated observations of individual SSA through the TEM, STEM, and nanoSIMS provided direct evidence of the occurrence of sulfate and nitrate in aged SSA in the arctic atmosphere.”

We have revised the text in section 5 as follows:

“NanoSIMS technology has been employed to obtain secondary ion intensity mappings of $^{12}C^-$, $^{16}O^-$, $^{12}C^{14}N^-$, $^{14}N^{16}O_2^-$, $^{32}S^-$, $^{35}Cl^-$, and $^{23}Na^{16}O^-$. $^{14}N^{16}O_2^-$ and $^{23}Na^{16}O^-$ mappings proved $NaNO_3$ formation in fully aged SSA.”

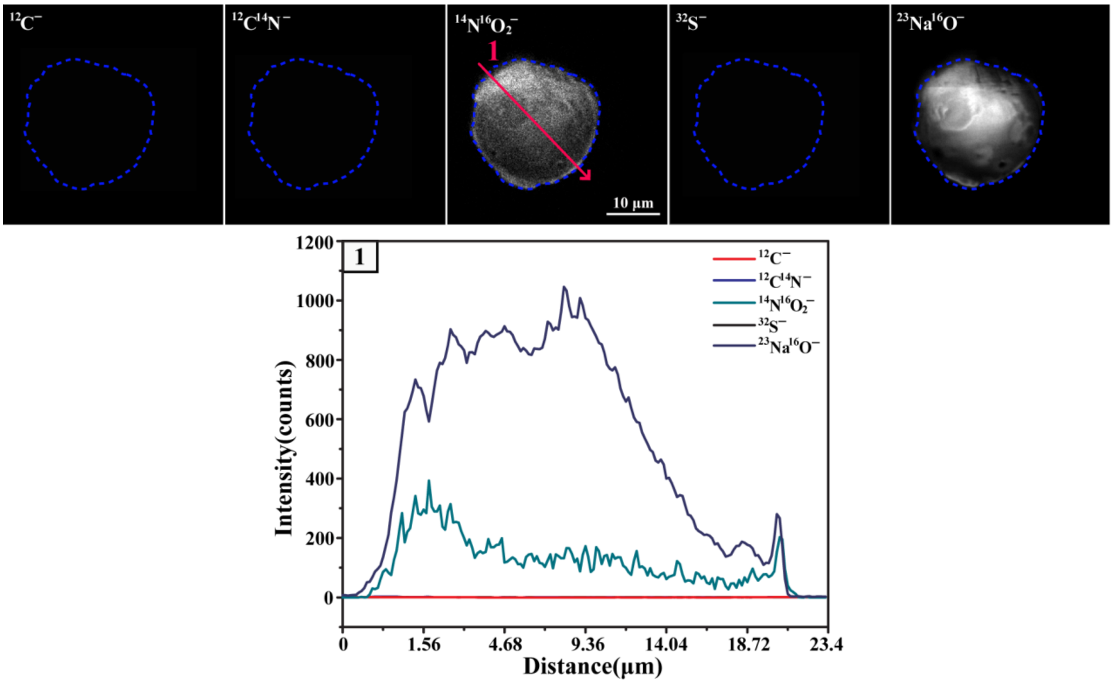

Figure S3. NanoSIMS-based ion intensity mappings. Mappings of $^{12}C^-$, $^{12}C^{14}N^-$, $^{14}N^{16}O_2^-$, $^{32}S^-$, and $^{23}Na^{16}O^-$ from laboratory generated $NaNO_3$ particle on silicon substrate. Line 1 represents the line scanning on the surface of individual particle.

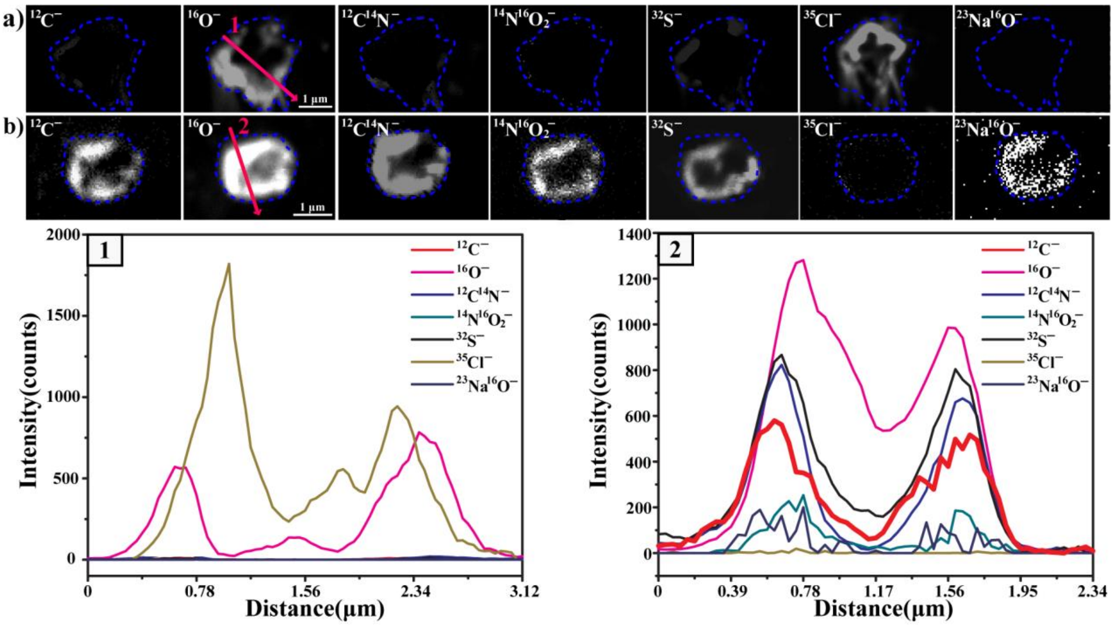

Figure 9. NanoSIMS-based ion intensity mappings. Mappings of $^{12}C^-$, $^{16}O^-$, $^{12}C^{14}N^-$, $^{14}N^{16}O_2^-$, $^{32}S^-$, $^{35}Cl^-$, and $^{23}Na^{16}O^-$ from one fresh SSA particle (a) and one fully aged SSA (b). Lines 1-2 represent the line scanning on the surfaces of individual particles. The red line represents the profile of $^{12}C^-$ in fully aged SSA.

2. Similar to nitrate, I am also wandering the occurrence of organic. The authors used $^{12}C^{14}N^-$ as an organic tracer. It seems to me that $^{12}C^{14}N^-$ may be a tracer of organonitrate or some specific types of organic, although I am not familiar with the technique. Please specify the availability of $^{12}C^{14}N^-$ as an organic tracer.

Response 2: We totally agree with the reviewer's comments. Similar to the question on nitrate, we did new nanoSIMS experiments including $^{12}C^-$ and $^{12}C^{14}N^-$ in SSA particles. We found $^{12}C^-$ and $^{12}C^{14}N^-$ ion intensity mappings have very similar distribution in individual particles. Based on the new experiment, we adopted $^{12}C^-$ as the tracer of organic matter. Figure 9 give some detail information of organic distribution following $^{12}C^-$ ion intensity mapping and line scan. We have revised "$^{12}C^-$" to replace "$^{12}C^{14}N^-$" in the appropriate text.

3. The authors classified sea-salt particles into fresh, partially aged, and fully aged ones based on morphology and chemical compositions. Is there any relation between the aging process and the back trajectory analysis? If not, it may not be appropriate to discuss compositional changes as particles age since the classification was made depending on the compositions but not aging, i.e., "it is shown that there is a major change of their internal structure and composition as the particles ageing (page 16724 line 24)" is not accurate because the particles aging was determined based on their internal structure and composition. Overall, it should be more careful to discuss the aging process unless the classification was determined based on the "aging."

Response 3: As the reviewer's requests, we re-analyzed the back trajectory. We found the particle ageing associated with the back trajectories of air masses. Please noticed that we revised Figure 6 and added new section 3.3 as follows:

"**3.3 The SSA aging and back trajectories of air masses**

Three-day (72h) back trajectories of air masses were generated using the HYSPLIT model at the Chinese Arctic Yellow River Station during August 3-23, 2012, at an altitude of 500 m above the sea level (Fig. 6). Most air masses originate in the Arctic Ocean, and are restricted to this vast marine region during the sampling periods. Figure 6 shows that two groups of back trajectories exhibit different ageing degree of SSA: One group originates from central Arctic Ocean and other one from North America and Greenland. Fractions of the fresh, partially aged, and fully aged SSA are 43.07%, 44.53%, and 12.41% in first group and 18.72%, 47.45%, 33.83% in second group, respectively (Fig. 6). As a result, air masses from North America and Greenland brought large amounts of aged SSA into the arctic area in summertime."

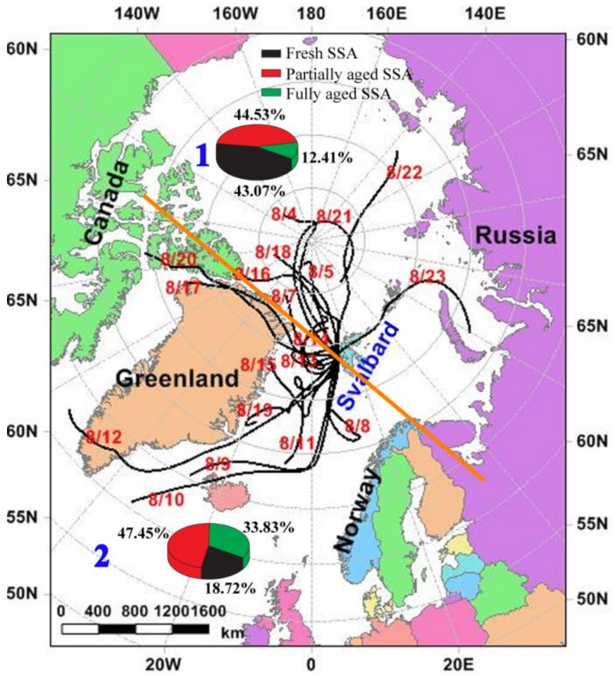

Figure 6. 72-h back trajectories of air masses at 500 m over Arctic Yellow River Station in Svalbard during 3-23 August, 2012, and arriving time was setting according to the sampling time. Air masses were divided into two groups by the yellow line: one group from central Arctic Ocean and other one from North America and Greenland. Pie charts showed the number fractions of the fresh, partially aged, and fully aged SSA.

We have revised the text (Page 16724, line 24) as follows:

"Using individual particle analysis of the three types of SSA, it is shown that there is a major change of their internal structure and composition"

4. Page 16715 Name and e-mail may not be consistent in the first corresponding author.

Response 4: It is our negligence and we are sorry about this. We have revised the text (Page 16715, Name and e-mail).

5. Page16718 Line 5: Recently, Laskin et al. (2012): : :. Here and elsewhere, authors refer Laskin et al. (2012). I suggest taking out "Recently" since it was published in 2012.

Response 5: Page16718 Line 5, Page16725 Line 22, and Page16727 Line 25, we delete “Recently” in the sentence.

6. Page16721 Line 21 (equation 1): I guess this equation is wrong (take out 4/3).

Response 6: We have revised the text (Page16721, Line 21) as follows:

$$A=\frac{4}{3}\pi r^2=\frac{\pi d^2}{3}\rightarrow d=\sqrt{\frac{3A}{\pi}} \qquad (1)$$

7. Page 16729 line 11: “Comparisons of fresh and aged SSA in Fig. 8 suggest that these organic coatings likely took part in the chloride depletion during particles ageing.” In Fig. 8 (and Fig. 7) authors show particle elemental mappings to show particle aging. However, they are different particles and do not show their aging process directly. Thus, the increasing or decreasing of elements may not reflect the aging process but just particle differences. Thus, it may be too strong to conclude “The chloride depletion in the SSA induced by the presence of organic matter should be incorporated into the atmospheric chemistry models for clean marine air (Page 16730 line 22)” from this study. At least, more careful discussion will be needed.

Response 7: We carefully made discussion as the reviewer’s comments. In this study, we carefully evaluated our data and back trajectories of air masses. Only the chloride depletion in the SSA can provide the direct evidence about the particle ageing in this study. As a result, the additional sulfate, nitrate, and organic matter were added in aged SSA. Based on laboratory experiments and our analysis, the heterogeneous reactions on SSA with acids can be explained the phenomenon. In the laboratory experiments, H_2SO_4/SO_2, HNO_3/NO_x, and organic acids can react with NaCl particles (Laskin et al., 2003;Ault et al., 2013;Ghorai et al., 2014). To make solid conclusion, we make one new Na-Cl-O triangular diagram in Figure 5. Figure 5 gives general information about Cl depletion of the fresh, partially aged, and fully aged SSA. Three particle types in the triangular diagram display interesting distribution: the fresh SSA around the NaCl, the partially aged SSA in the center of triangular (including partial NaCl), the fully aged SSA around $NaNO_3$ and Na_2SO_4 (chloride full depletion).

We have revised the text in section 3.3 and 4.1 as follows:

"To summarize three types of SSA, we make one Na-Cl-O triangular diagram. Figure 5 gives general information about Cl depletion among the fresh, partially aged, and fully aged SSA. Three particle types in the triangular diagram display interesting distribution: the fresh SSA around the NaCl, the partially aged SSA in the center of triangular (including partial NaCl), the fully aged SSA around $NaNO_3$, and Na_2SO_4 (chloride full depletion)."

"Na-Cl-O triangular diagram further shows that Cl in SSA has been depleted and O content increases likely through additional chemical reactions (Fig. 5)."

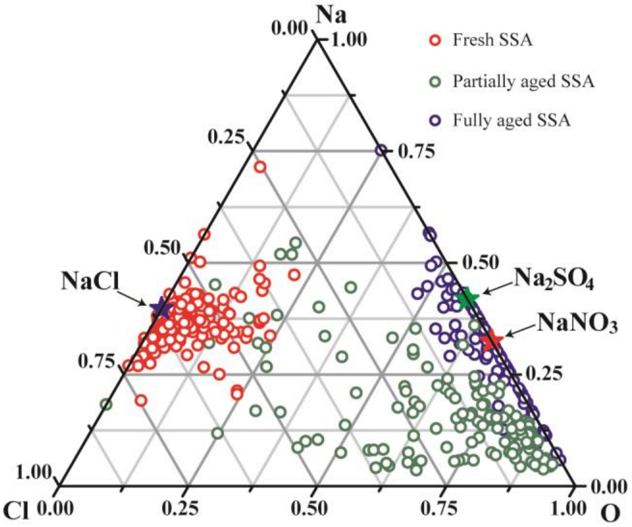

Figure 5. Triangular diagram of Na-Cl-O showing EDX data of elemental composition of 405 SSA. Three stars represent elemental composition of pure NaCl, Na_2SO_4, and $NaNO_3$, respectively.

8. Figure 3: Fig. 3j shows O signal for $MgCl_2$ in EDX but Fig. 3k does not have O for CaSO4. Why?

Response 8: Because $MgCl_2$ is close to $CaSO_4$ in the individual particle, O signal in $MgCl_2$ is from the nearby $CaSO_4$. For O signal in $CaSO_4$, it is our negligence and we are sorry about this. We selected suitable EDX data of $MgCl_2$ and $CaSO_4$ in Figure 2 as follows:

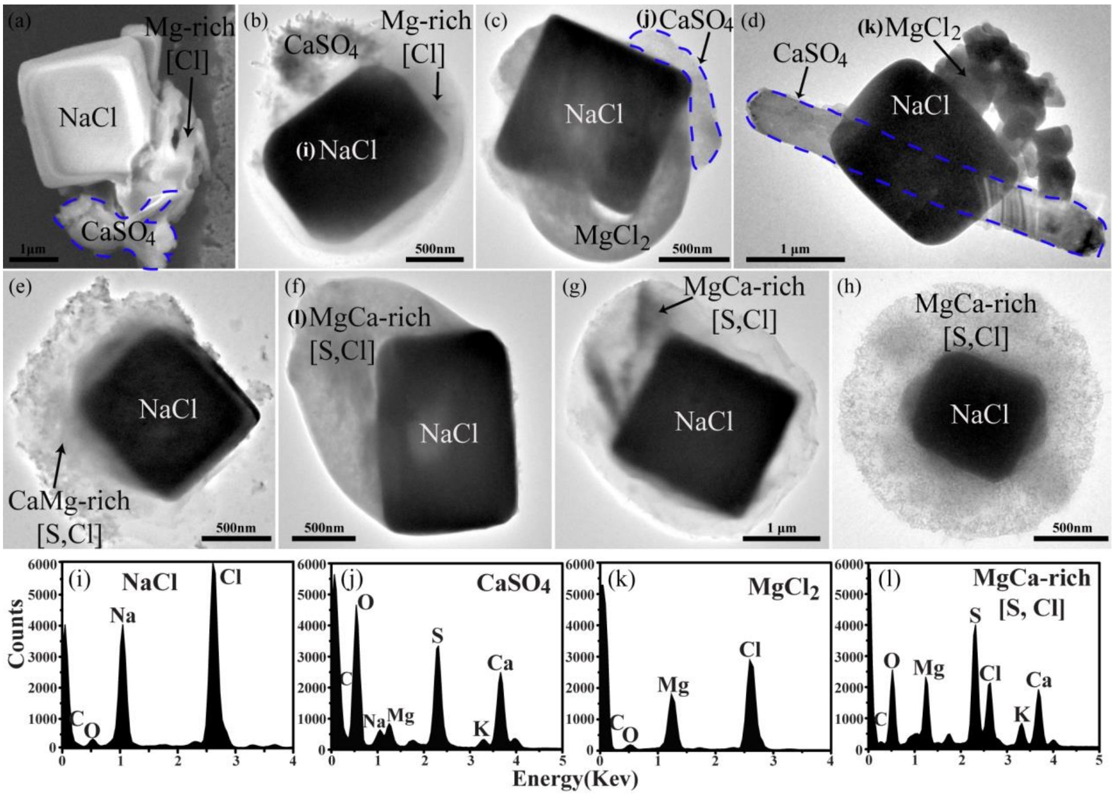

Figure 2. Morphology and EDX spectra of the typical fresh SSA. (a) One SEM image, (b)-(h) TEM images, and (i)-(h) EDX spectra of NaCl, $MgCl_2$, $CaSO_4$, and MgCa-rich. The main anionic elements are shown in the square brackets.

9. Please specify the cutoff size in aerodynamic diameter for the sampler if any. The cutoff sizes will influence the particle size distributions.

Response 9: We have revised the text in section 2.1 as follows:

"The collection efficiency of the impactor is 50% for particles with an aerodynamic diameter of 0.3 μm and almost 100% at 0.5 μm if the density of particles is 2 g cm^{-3}"

10. N mapping may be artifact since it was determined without detecting N in EDX. It can come from C and O since N peak is between these elements. Please check it. The TEM images are rotated comparing to the mapping images. Can it be fixed?

Response 10: We didn't fully understand the reviewer's comments. We try to answer them. In the EDX spectra, we could not determine N signal (Figs. 2-4). However, we can obtain the N mapping in the scanning TEM (Fig. 8). In the dark-field mode of

TEM, there is the lowest noise and highest resolution for light element. Therefore, N mapping is believable in Figure 8, although it cannot supply the quantitative data. Fortunately, we had new nanoSIMS experiments to provide direct evidence about the nitrate (Figs. 9 and S3).

11. Figure S2: Please check if the R^2 value is correct. It looks the value (R^2=0.9888) is too high for the plotting.

Response 11: We checked the R^2. Previously, we used OriginPro 8 to process the AFM data, R^2=0.9888. We used microsoft excel 2010 to calculate it again. The value is R^2=0.765. We thank the reviewer’s comments.

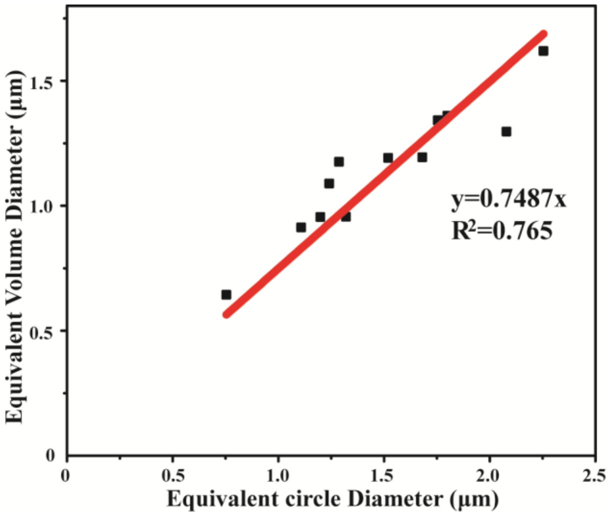

Figure S2. The correlation of equivalent circle diameter (d) and equivalent volume diameter (D) obtained by AFM.

References:

Ault, A. P., Guasco, T. L., Ryder, O. S., Baltrusaitis, J., Cuadra-Rodriguez, L. A., Collins, D. B., Ruppel, M. J., Bertram, T. H., Prather, K. A., and Grassian, V. H.: Inside versus outside: ion redistribution in nitric acid reacted sea spray aerosol particles as determined by single particle analysis, J. Am. Chem. Soc., 135, 14528-14531, doi:10.1021/ja407117x, 2013.

Ghorai, S., Wang, B., Tivanski, A., and Laskin, A.: Hygroscopic properties of internally mixed particles composed of NaCl and water-soluble organic acids, Environ. Sci. Technol., 48, 2234-2241, doi:10.1021/es404727u, 2014.

Laskin, A., Gaspar, D. J., Wang, W. H., Hunt, S. W., Cowin, J. P., Colson, S. D., and Finlayson-Pitts, B. J.: Reactions at interfaces as a source of sulfate formation in sea-salt particles, Science, 301, 340-344, 2003.